Ammonia synthesis over multi-promoted iron catalysts obtained by high-energy ball-milling

Claus J.H. Jacobsen [a,*], Jianzhong Jiang [b], Steen Mørup [b], Bjerne S. Clausen [a] and Henrik Topsøe [a]

[a] *Haldor Topsøe Research Laboratories, Nymøllevej 55, DK-2800 Lyngby, Denmark*
[b] *Department of Physics, Building 307, Technical University of Denmark, DK-2800 Lyngby, Denmark*

Received 8 April 1999; accepted 28 June 1999

The feasibility of producing ammonia synthesis catalysts from high-energy ball-milling of a simple mixture of the constituent oxides has been investigated. The effect of ball-milling the fused oxidic precursor of the industrial KM1 ammonia synthesis catalyst has also been studied. The results show that high-energy ball-milling offers some interesting possibilities for preparing novel catalytic materials. It is observed that ball-milling of the powder oxides mixture leads to formation of solid solutions and the catalytic activity is significantly higher than that of the starting material. Furthermore, ball-milling of fused oxidic KM1 precursor is seen to give rise to more homogeneous promoter distribution and slightly higher activity. The quite small activity increase observed in this case probably reflects the fact that the fusion process has already resulted in a close to optimal promoter distribution. The choice of atmosphere during ball-milling is also seen to offer possibilities for regulating the phase composition.

Keywords: catalytic ammonia synthesis, iron catalyst, high-energy ball-milling

1. Introduction

The industrial multi-promoted iron catalyst for catalytic ammonia synthesis has almost exclusively been produced by fusion of oxides followed by reduction. This catalyst has been subject to numerous studies and over the years several new techniques, methods and theories of catalysis have initially been applied to this system. Both the preparation and activation [1], the structure, surface chemistry and kinetics [2] of the industrial iron catalyst have been comprehensively reviewed. Typically, the oxidic precursor structure formed after melting of a mixture of iron and promoter oxides contains iron in both magnetite, wüstite and calcium ferrites. In general, the grain boundaries formed after solidifying the melt are found to contain much higher concentrations of the promoters than the magnetite [3]. Mössbauer spectroscopic studies have revealed that during activation wüstite reduces to metallic iron prior to magnetite reduction [4]. After activation both aluminum and calcium are present in their oxidic states and are considered structural promoters. Potassium is an electronic promoter, but its formal oxidation state has not been conclusively established under industrial conditions.

Preparation of the fused multi-promoted iron catalyst involves fusion of suitable precursors and solidification of the resulting melt by cooling, as mentioned above. After crushing and sizing, the catalyst may be reduced and passivated by controlled oxidation to allow handling of the catalyst under ambient conditions. Each of the steps involved in the manufacturing process has been shown to critically influence the final activity of the catalyst. The chemical composition of the oxidic catalyst precursor and the distribution of the promoters are largely governed by the choice of precursors and the detailed conditions of the fusion and cooling processes. In many respects, it would be ideal to achieve a very homogeneous distribution of the promoters in the oxidic catalyst precursor in order to obtain an optimum coverage of the promoters on all iron crystals. In practice this is not possible by the fusion–cooling process since all the components are not mutually soluble and phase segregation occurs to various extents during solidification. Recently, it has been shown that high-energy ball-milling can be used to synthesise quite homogeneous materials far from equilibrium. Some examples are amorphous alloys, nanostructured materials, and metastable solid solutions [5–8]. In this process, powder particles are subjected to severe mechanical deformation during collisions with balls and vial and are repeatedly deformed, cold welded and fractured, so that solid-state reactions and/or mechanochemical reactions in powder mixtures can be induced. The advantage of this technique is that it can be used to directly prepare nanostructured powders at ambient temperature. Recently, high-energy ball-milling has been applied in the preparation of various inorganic catalysts [9–16], e.g., Cu/ZnO catalysts for methanol synthesis [9], iron oxide catalysts for Fischer–Tropsch synthesis [10], TiO_2/MO_3 (M = W and Mo) catalysts for removing nitrogen oxides from flue gases [11], binary CeO_2–MO_2 (M = Zr, Hf, and Tb) solid solutions for oxygen storage/transport [12], and mixed VPO/Bi_2O_3 and VPO/$BiPO_4$ oxidation catalysts [13]. The present study has explored possibilities of preparing new ammonia synthesis catalysts and in particular enhancing the catalytic activity of an in-

* To whom correspondence should be addressed.

dustrial catalyst, the Haldor Topsøe KM1 catalyst, by high-energy ball-milling.

2. Experimental

2.1. Ball-milling

An industrial ammonia synthesis catalyst consists mainly of iron oxides (95 wt%) together with small amounts of promoters such as Al_2O_3, CaO, K_2O, and MgO. For the ball-milling experiments, two starting materials were used, one is a Haldor Topsøe KM1 ammonia synthesis catalyst and the other a mixture of pure oxide powders corresponding to the composition of KM1. The milling was carried out using a planetary ball-mill (Fritsch Pulverisette 5), in both *open* containers (i.e., the valves on the lid were open to the atmosphere during the milling) and *closed* containers (i.e., the valves on the lid were closed during the milling but no attempt was made to avoid air during charging of the container with solid material). The vials and balls were made of hardened stainless steel (containing about 18 wt% Cr and 8 wt% Ni). The milling intensity was 200 rotations per minute, and a ball-to-powder weight ratio of 20 : 1 was chosen. The milling process was interrupted after selected times to remove small amounts of powder for analysis. The composition of the milled samples was examined by scanning electron microscopy with an energy dispersive X-ray analysis facility. It was found that the Cr contamination originating from the abrasion of the vials and balls in samples milled for the longest time (110 h) was less than 1 at%.

2.2. X-ray powder diffraction (XRPD)

X-ray diffraction patterns were recorded by slow scanning on a Philips vertical goniometer equipped with a θ-compensating divergence slit and a diffracted beam monochromator utilizing Cu Kα radiation. All crystal sizes were calculated from the line broadening using the Scherrer equation assuming that the broadening exclusively origins from size effects.

2.3. Transmission electron microscopy (TEM)

TEM micrographs from selected samples were obtained using a Philips EM430 TEM (300 keV).

2.4. Mössbauer spectroscopy

Mössbauer spectra were recorded with a conventional constant-acceleration spectrometer in transmission geometry with sources of about 25 mCi ^{57}Co in a Rh matrix. Isomer shifts are given relative to that of α-Fe at room temperature. A closed-cycle helium cryostat was used for low-temperature Mössbauer measurements.

2.5. N_2 adsorption/desorption

Surface areas of the oxidic catalysts were obtained from dinitrogen adsorption and desorption using a Quantachrome Autosorb analyser.

2.6. Ammonia synthesis

The catalytic activity for ammonia synthesis was determined using the high-pressure set-up described by Nielsen [3]. In brief, the set-up consists of an isothermal reactor with a catalyst bed of 8 mm internal diameter and 50 mm length operated at 410 °C and a pressure of 100 bar. The inlet gas contained 4.5% ammonia in 3 : 1 H_2/N_2 and the flow was adjusted to obtain 12% ammonia in the outlet. The ball-milled samples were pressed into tablets and crushed to a particle size of 0.3–0.8 mm prior to testing. Under these conditions the rate measurements were free of mass and heat transfer limitations. The ammonia inlet and outlet concentrations were determined with a BINOS detector. The reported catalytic activities are based on the mass of catalyst present in the reduced state, thereby taking the variations in oxygen contents into account. The activities are reported in units of normal liters of ammonia produced per hour per gram of catalyst. The catalysts were activated by heating 3.0 g of oxidic catalyst at 0.05 °C/min from room temperature to 500 °C in a flow of 50 l/h synthesis gas. The sample was kept at 500 °C for 36 h and cooled to 410 °C for measurement of catalytic activity. Water production during activation was monitored by gas chromatographic analysis and the concentration did not in any case exceed 3000 ppm.

3. Results

In table 1, selected properties of the KM1 catalysts prior to and after ball-milling for 40 and 110 h are shown. Furthermore, results obtained from the oxide mixture prior to and after 100 h milling are included.

3.1. Samples from ball-milled KM1

Initially, the KM1 catalyst is almost non-porous and contains magnetite with small amounts of wüstite and calcium ferrite, but it is seen that the surface area is significantly increased by the ball-milling procedure and this effect is most pronounced for the sample exposed to air during ball-milling. Figure 1 shows the X-ray powder diffraction patterns of samples removed from the ball-milling process at various times. In the closed container it is seen that the wüstite and calcium ferrite disappear and a reduction in crystal size is observed. For the sample exposed to air, the wüstite and calcium ferrite also disappear and a transformation of magnetite to hematite with a small average crystal size is observed. These findings are confirmed by the Mössbauer spectra obtained from the same samples and

Table 1
Selected properties of samples obtained by various ball-milling procedures.

	Prior to ball-milling	Ball-milling	
		40 h	110 h
KM1 closed			
BET (m^2/g)	0.008	3.9	3.4
Phases (XRPD)	Magnetite Wüstite Calcium ferrite	Magnetite	Magnetite
Crystal size (nm)	>1000 (magnetite)	5.6	5.7
KM1 open			
BET (m^2/g)	0.008	–	13.0
Phases (XRPD)	Magnetite Wüstite Calcium ferrite	Hematite Magnetite	Hematite
Crystal size (nm)	>1000 (magnetite)	11 (hematite)	10
Oxide mixture			100 h closed
BET (m^2/g)	0.32		6.9
Phases (XRPD)	Magnetite CaO Boehmite		Magnetite
Crystal size (nm)	>1000 (magnetite)		8.0

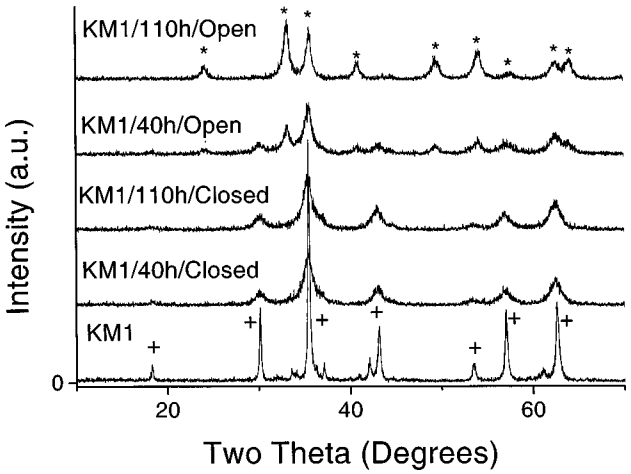

Figure 1. X-ray diffraction patterns of the KM1 sample and samples milled for 40 and 110 h in open and closed containers. (∗) Diffraction lines of hematite; (+) diffraction lines of magnetite.

shown in figure 2. The Mössbauer spectra obtained after milling with and without exposure to air for 1 h are very similar and show the presence of two sextets with Mössbauer parameters very similar to those of iron at the A and B sites in magnetite. The B-site component has broader lines than the corresponding component in pure magnetite. This is due to substitution of promoter cations (mainly Al^{3+}) into the magnetite phase. The spectra also contain a doublet with Mössbauer parameters typical for wüstite ($Fe_{1-x}O$) and with a relative spectral area of 14%. Upon further milling the powders milled in closed and open containers develop in different ways. In the closed container the magnetite-like component is present in all samples, but both the A-site and the B-site lines become very broad after extended milling. Furthermore, the doublet due to wüstite gradually disappears. The spectra of the sample milled for 110 h, obtained at 80 and 15 K (figure 3), show a change in the spectral shape similar to that seen in pure magnetite above and below the Verwey transition, respectively. It appears that the Verwey transition in the ball-milled catalyst takes place at about 80 K. Ball-milling in the open container is seen to result in a gradual disappearance of the magnetite components and instead a hematite (α-Fe_2O_3) component with broad lines appears. This shows that oxidation has taken place and the results are in agreement with previous studies of ball-milled iron oxides [17]. The spectrum of the sample milled for 110 h, obtained at 80 K, shows, however, a residual component with low intensity and with parameters similar to magnetite (figure 3). Thus, the magnetite has not transformed completely to hematite after 110 h ball-milling. Transmission electron micrographs from the samples milled for 110 h in closed and open containers show the presence of small crystals of magnetite and hematite, respectively.

3.2. Samples from ball-milled oxide mixture

The Mössbauer spectra of the ball-milled mixture of pure oxides in a closed container are shown in figure 4. As expected, the spectrum obtained after 1 h is essentially identical to that of pure magnetite. Upon further milling the lines are broadened but the spectra still show the features typical for magnetite, i.e., the presence of two sextets with different isomer shifts and magnetic hyperfine fields. After ball-milling for 100 h the line broadening is, however, less pronounced than that seen in the spectra of the ball-milled KM1 catalyst after extended ball-milling. Similarly, the XRPD patterns show the presence of magnetite. Thus, the results indicate that a completely homogeneous structure has not been achieved yet. After the ball-milling for 100 h the crystal size is estimated to be approximately 8.0 nm.

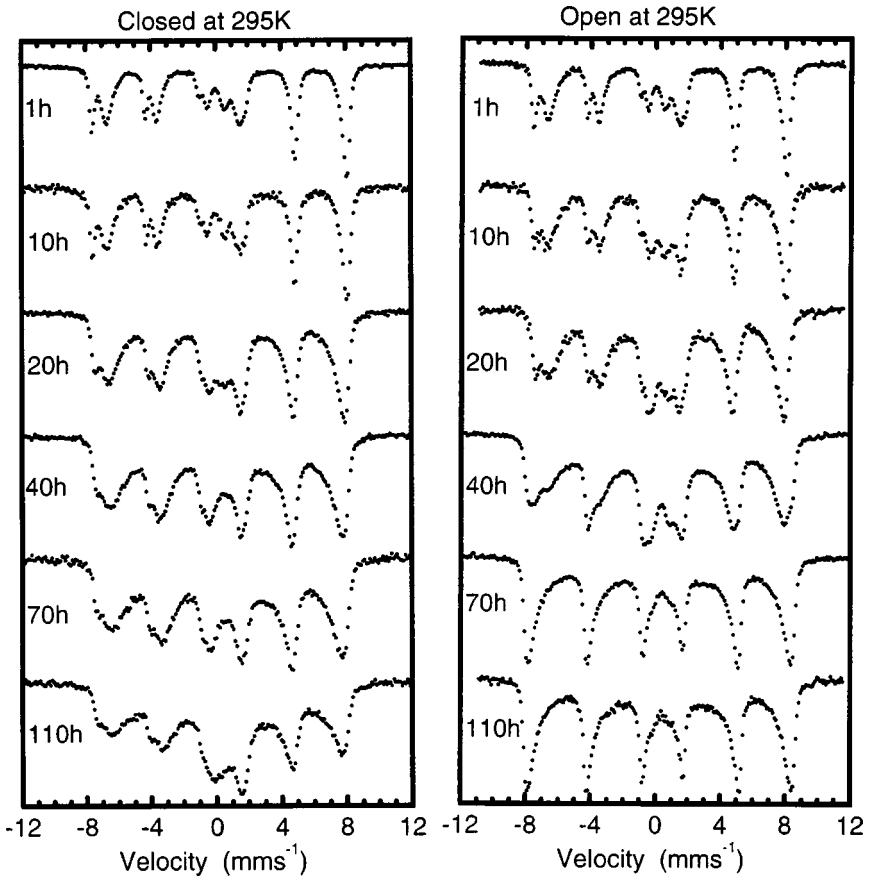

Figure 2. Room-temperature Mössbauer spectra of KM1 samples milled for various times in open and closed containers.

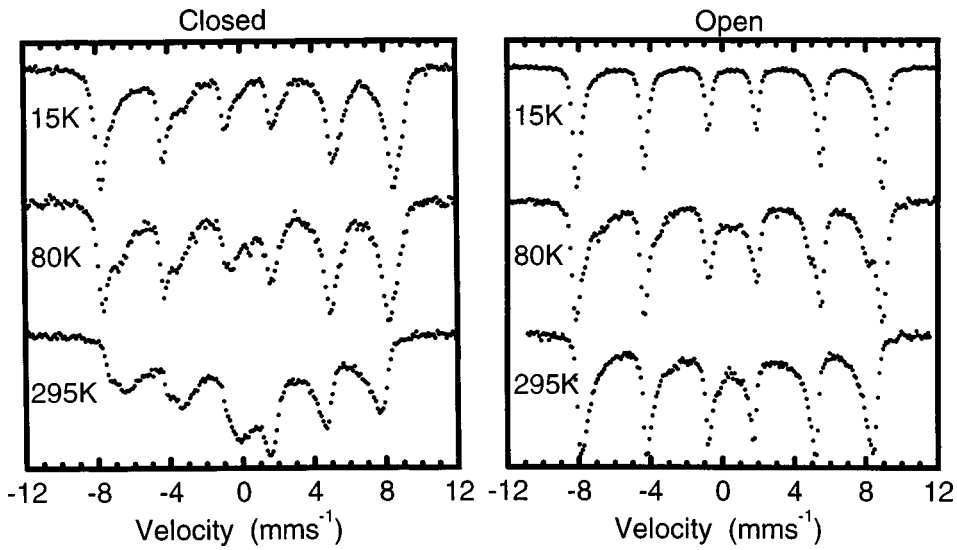

Figure 3. Low-temperature Mössbauer spectra of the KM1 sample milled for 110 h in open and closed containers.

3.3. Catalytic activity

In table 2, the catalytic activities of the samples tested are summarised. It is seen that the ball-milling procedure only results in a slight increase of the catalytic activity of KM1. Both the samples ball-milled with and without exposure to air have a marginally higher catalytic activity on a weight basis compared to KM1. Due to the significantly higher porosity of the ball-milled catalysts the volume activities are lower than KM1. On the other hand, the catalyst prepared by ball-milling of the constituent oxides for 100 h has an activity which is considerably higher than that of a sample prepared by simply mixing the constituent oxides. After testing, the catalyst samples were all characterised by

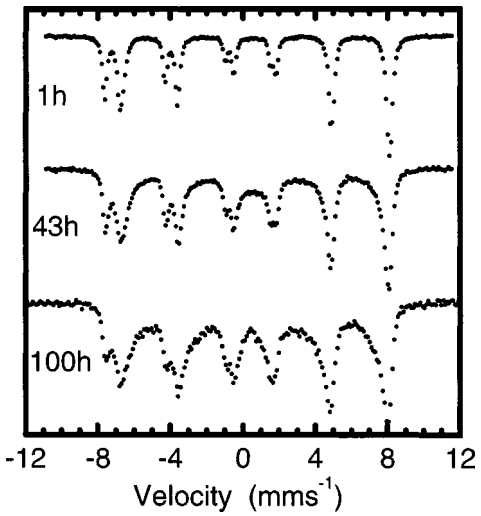

Figure 4. Room-temperature Mössbauer spectra of the mixture of pure oxides after various milling times in a closed container.

Table 2
Catalytic activity for ammonia synthesis at $T = 410\,^{\circ}\mathrm{C}$ and $p = 100$ bar in 3 : 1 mixture of $H_2 : N_2$ containing ca. 8% ammonia.

Sample	Ammonia production ($\mathrm{Nl\,h^{-1}\,g^{-1}}$)	Apparent density (g/ml)
KM1	0.75	2.8
KM1 ball-milled		
110 h closed	0.78	2.1
110 h open	0.78	2.2
Oxide mixture		
ball-milled 100 h	0.62	2.1
simple mixture	0.13	2.0

XRPD. In all the samples of KM1 catalysts, only metallic iron crystals could be detected with an average crystal size around 25 nm. For the catalyst prepared by ball-milling of the oxide mixture the iron crystals showed an average size of 35 nm.

4. Discussion

Both Mössbauer spectroscopy and X-ray powder diffraction show that the ball-milling has a dramatic influence on the structure of the KM1 catalyst. When the ball-milling is performed without exposure to air it appears that the primary result of the ball-milling is a reduction of the magnetite crystal size and a more homogeneous distribution of the promoter atoms. Since no correction for strain and inhomogeneity in solid solution is made, the crystal size estimated by the Scherrer equation is somewhat on the low size compared to that estimated from the transmission electron micrographs and the BET surface area. However, there is no doubt that very small magnetite crystals are achieved by the high-energy ball-milling procedure. Such small crystal sizes are not obtained by the fusion method. When the ball-milling is performed in air the magnetite crystals are observed to gradually transform into hematite, which is the thermodynamically stable iron oxide in air at low temperature. Also the hematite formed is seen to consist of small crystals. The Mössbauer spectra and XPRD patterns show that the samples milled in closed and open vials both seem to be more homogeneous after extended milling, i.e., the wüstite and calcium ferrite phases have disappeared and only magnetite and hematite phases substituted with promoter atoms can be detected after 110 h. A similar behaviour has been observed in other studies of ball-milled ceramics and metals and even if the solid solutions are thermodynamically unstable they can often be formed during milling from a mixture of powders [7,8]. The broad lines in the Mössbauer spectra of the ball-milled KM1 samples indicate that promoter cations have entered into the iron oxide phases. Another possible explanation of the Mössbauer line broadening could be that the small particle size results in relaxation of the magnetization vector. However, application of an external magnetic field only resulted in a change in the relative area of the absorption lines, but the line width was unchanged. Therefore, relaxation effects seem to play only a minor role for the line broadening [18]. It is somewhat surprising that although the ball-milled samples seem to have become more homogeneous at the atomic scale the catalytic activity is only slightly improved. This may indicate that enough textural promoters have entered the magnetite phase during melting to stabilize the small iron particles produced after reduction. The results also suggest that the final particle size of the iron crystals is not very sensitive to a reduction of the crystal size of the magnetite catalyst precursor.

The sample prepared by ball-milling the mixture of pure oxides is found to contain substituted magnetite after 100 h, but the Mössbauer line broadening is less pronounced than that found in the spectra of milled KM1 samples. This suggests that with the present conditions there is less substitution of promoter cations in the magnetite than achieved via the melting route followed by ball-milling. It appears plausible that this is the reason for the somewhat lower catalytic activity compared to KM1. Nevertheless, it is evident that the ball-milling has resulted in the introduction of promoters into the magnetite lattice. Furthermore, it is worth noticing that the present samples obtained by ball-milling of the raw materials have a catalytic activity which is higher than that reported in literature for many iron-based catalysts. For comparison, Tennison [19] reports the activity of a triply promoted iron catalyst to be ca. 60 kmol $NH_3\,h^{-1}\,m^{-3}$ at an average ammonia concentration of 8%, 430 °C and 138 bar. At a significantly lower temperature and pressure (410 °C and 100 bar) our ball-milled catalyst produces exactly the same amount of ammonia. Therefore, the results show that catalysts with high activity can be obtained using ball-milling and this method may be developed into an alternative to the fusion method. Clearly, further optimisation of the procedures should be possible. Currently, it appears that the primary obstacle in obtaining interesting ammonia synthesis catalysts for com-

mercial operation is related to the significantly lower density of these materials.

5. Conclusion

The results show that high activity ammonia synthesis catalysts can be produced by ball-milling simple mixtures of iron oxides and promoter oxides. The structural investigations show that the ball-milling results in significant size reduction and the introduction of promoter oxides into the magnetite lattice. In case of ball-milled samples prepared from fused KM1, the catalytic activities of the ball-milled catalysts are only slightly improved compared to that of KM1. It is likely that other parameters (e.g., the amount of promoters, the activation procedure, etc.) have to be modified in order to prepare ball-milled catalysts with the optimal activity using either a mixture of oxides or a fused catalyst as a starting material.

Acknowledgement

This work was financially supported by the Danish Technical Research Council. Particular thanks go to Poul Lenvig Hansen for his assistance by TEM measurements.

References

[1] R. Schlögl, in: *Catalytic Ammonia Synthesis – Fundamentals and Practice*, ed. J.R. Jennings (Plenum, New York, 1991) p. 19.
[2] P. Stoltze, in: *Ammonia – Catalysis and Manufacture*, ed. A. Nielsen (Springer, Berlin, 1995) p. 16.
[3] A. Nielsen, *An Investigation on Promoted Iron Catalysts for the Synthesis of Ammonia*, 3rd Ed. (Jul. Gjellerup, 1968).
[4] B.S. Clausen, S. Mørup, H. Topsøe, R. Candia, E.J. Jensen, A. Baranski and A. Pattek, J. Phys. Colloq. 37 (1976) C6-245.
[5] W.L. Johnson, Prog. Mater. Sci. 30 (1986) 81.
[6] C.C. Koch, in: *Materials Science and Technology*, Vol. 15, eds. R.W. Cahn, P. Haasen and E.J. Kramer (VCH, Weinheim, 1991) p. 193.
[7] J.Z. Jiang, C. Gente and R. Bormann, Mater. Sci. Eng. A 242 (1998) 268.
[8] J.Z. Jiang, R. Lin, S. Mørup, K. Nielsen, F.W. Poulsen, F.J. Berry and R. Clasen, Phys. Rev. B 55 (1997) 11;
J.Z. Jiang, S. Mørup and S. Linderoth, Mater. Sci. Forum 225–227 (1996) 489;
J.Z. Jiang, R.K. Larsen, R. Lin, S. Mørup, I. Chorkendorff, K. Nielsen, K. Hansen and K. West, J. Solid State Chem. 138 (1998) 114.
[9] L. Huang, G.J. Kramer, W. Wieldraaijer, D.S. Brands, E.K. Poels, H.L. Castricum and H. Bakker, Catal. Lett. 48 (1997) 55.
[10] T. Rühle, D. Herein, N. Pfander, G. Weinberg, T. Braum and R. Schlögl, Oral presentation at XXIX Jahrestreffen deutscher Katalytiker, Friedrichroda, 20–22 March 1996.
[11] F.C. Jentoft, H. Schmelz and H. Knözinger, Appl. Catal. A 161 (1997) 167.
[12] A. Trovarelli, F. Zamar, J. Llorca, C. de Leitenburg, G. Dolcetti and J.T. Kiss, J. Catal. 169 (1997) 490;
A. Trovarelli, P. Matteazzi, G. Dolcetti, A. Lutman and F. Miani, Appl. Catal. A 95 (1993) L9;
F. Zamar, A. Tovarelli, C. de Leitendam and G. Dolcetti, in: *11th Int. Congr. on Catalysis*, Stud. Surf. Sci. Catal., Vol. 101B, eds. J.W. Hightower, W.N. Delgass, E. Iglesia and A.T. Bell (Elsevier, Amsterdam, 1996) p. 1283.
[13] V.A. Zazhigalov, J. Haber, J. Stoch, L.V. Bogutskaya and I.V. Bacherikova, Appl. Catal. A 135 (1996) 155;
V.A. Zazhigalov, J. Haber, J. Stoch, L.V. Bogutskaya and I.V. Bacherikova, in: *11th Int. Congr. on Catalysis*, Stud. Surf. Sci. Catal., Vol. 101B, eds. J.W. Hightower, W.N. Delgass, E. Iglesia and A.T. Bell (Elsevier, Amsterdam, 1996) p. 1039.
[14] M. Crocker, R.H.M. Herold, C.A. Emeis and M. Krijger, Catal. Lett. 15 (1992) 339.
[15] S. Mori, W.C. Xu, T. Ishidzuki, N. Ogasawara, J. Imai and K. Kobayashi, Appl. Catal. A 137 (1996) 255.
[16] L.T. Weng, N. Spitaels, B. Yasse, J. Ladrire and P. Ruiz, J. Catal. 132 (1991) 319.
[17] J.Z. Jiang, Y.X. Zhou, S. Mørup and C.B. Koch, Nanostruct. Mater. 7 (1996) 401;
S. Linderoth, J.Z. Jiang and S. Mørup, Mater. Sci. Forum 235–238 (1997) 205.
[18] S. Mørup, B.S. Clausen and P.H. Christensen, J. Magn. Magn. Mater. 68 (1987) 160.
[19] S.R. Tennison, in: *Catalytic Ammonia Synthesis – Fundamentals and Practice*, ed. J.R. Jennings (Plenum, New York, 1991) p. 305 (see figure 9.1(b)).